# Electronic Supplementary Information (ESI)

## Can multi–biaxial mesogenic mixtures favour biaxial nematics? A computer simulation study

Lara Querciagrossa, Matteo Ricci, Roberto Berardi(*) and Claudio Zannoni
*Department of Industrial Chemistry "Toso Montanari",*
*University of Bologna, viale Risorgimento 4, 40136 Bologna, Italy*

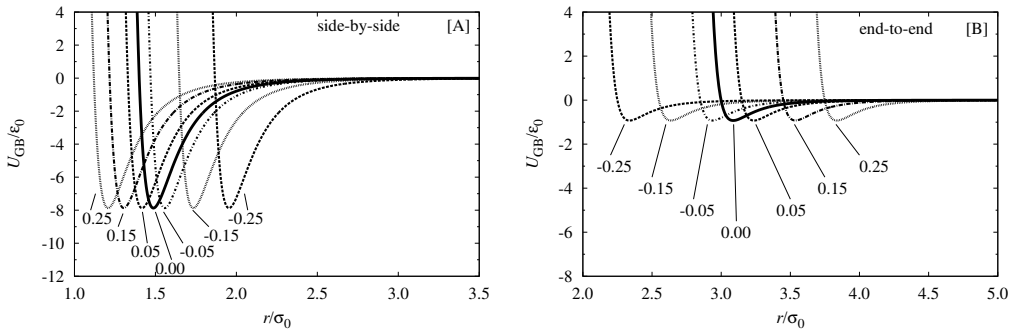


Figure S1: The homogeneous *side–by–side* and *end–to–end* pair potential energy profiles for some of the various GB ellipsoids (the cutoff radius is $r_c = 5\ \sigma_0$).

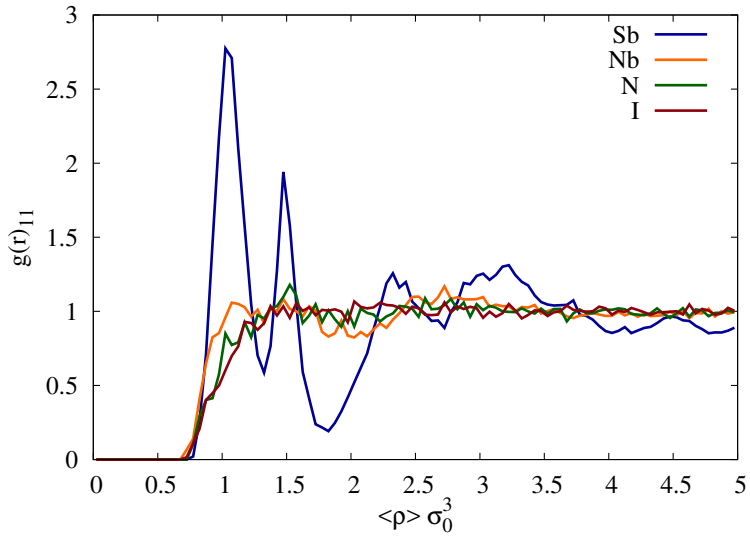


Figure S2: Representative radial correlation functions for the $s = 0.00$ species in the isotropic I, nematic N, biaxial nematic $N_b$, and biaxial smectic $S_b$ phases observed for the $s_{max} = 0.20$ sample.

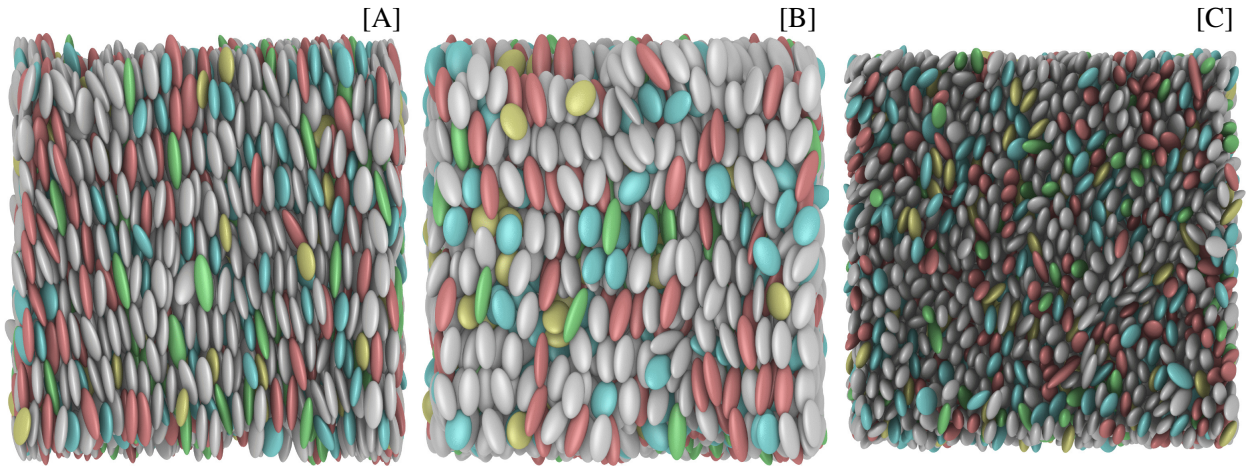


Figure S3: Snapshots of the $N_b$ phase at $T^* = 2.5$ for the $s_{max} = 0.20$ sample. The three views have been taken along the **l** (plate A), **m** (plate B), and **n** (plate C), directors. Particles have been colour coded according as $s = -0.20$ yellow, $s = -0.15$ cyan, $s = 0.00$ gray, $s = 0.15$ pink, $s = 0.20$ green.

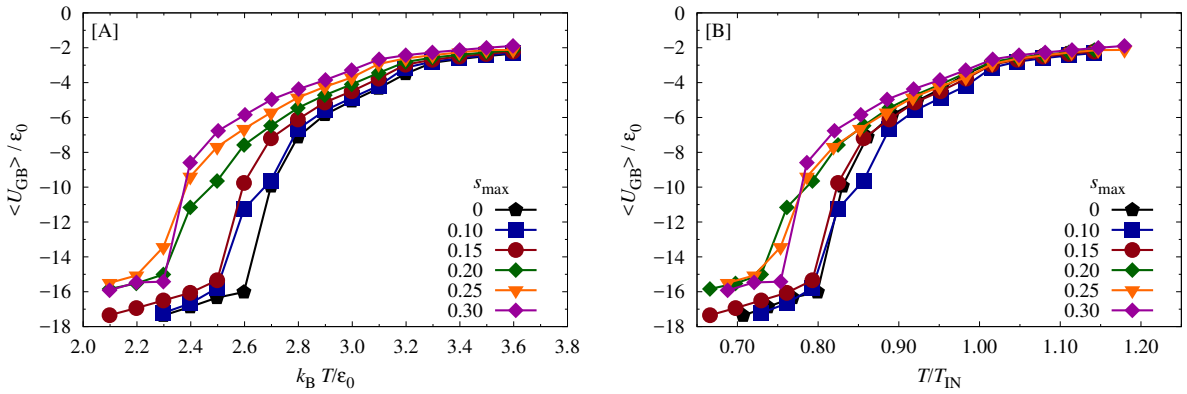


Figure S4: The average potential energy per particle $\langle U_{\mathrm{GB}} \rangle$ at various dimensionless (plate A), and reduced (plate B) temperatures for the five non–uniform mixtures with $s_{\mathrm{max}} = 0.10$ (blue squares), 0.15 (red circles), 0.20 (green diamonds), 0.25 (orange triangles), and 0.30 (purple diamonds). The data for the reference system with $s_{\mathrm{max}} = 0.00$ (black pentagons) are also plotted.

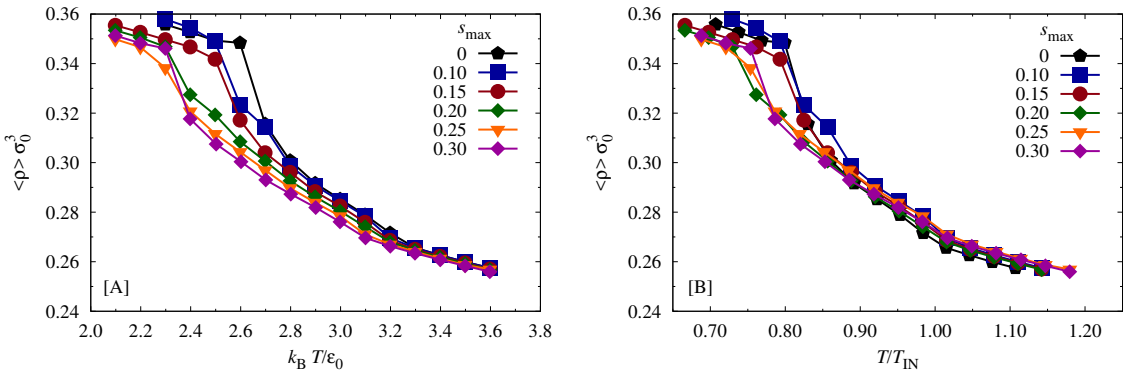


Figure S5: The average number density $\langle \rho \rangle$ at various dimensionless (plate A), and reduced (plate B) temperatures for the five non–uniform mixtures. See caption of Figure S4 for further details.

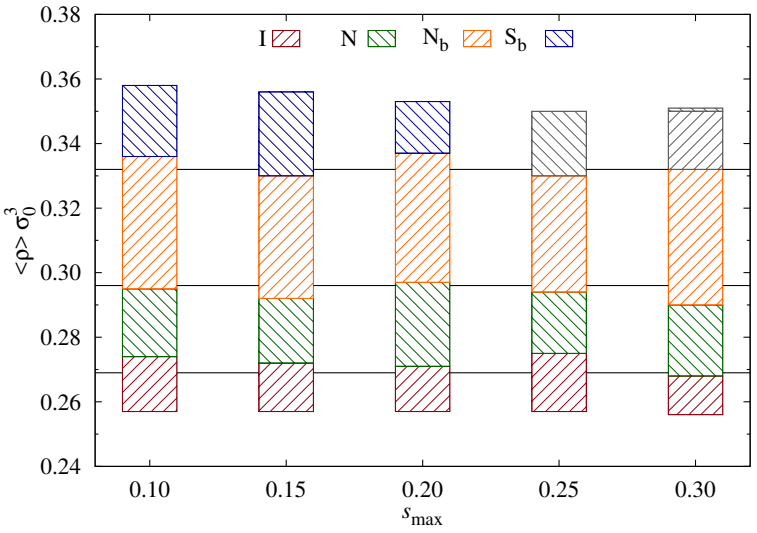


Figure S6: The phase sequence observed with respect to the average number density values. See caption of Figure 4 for details.

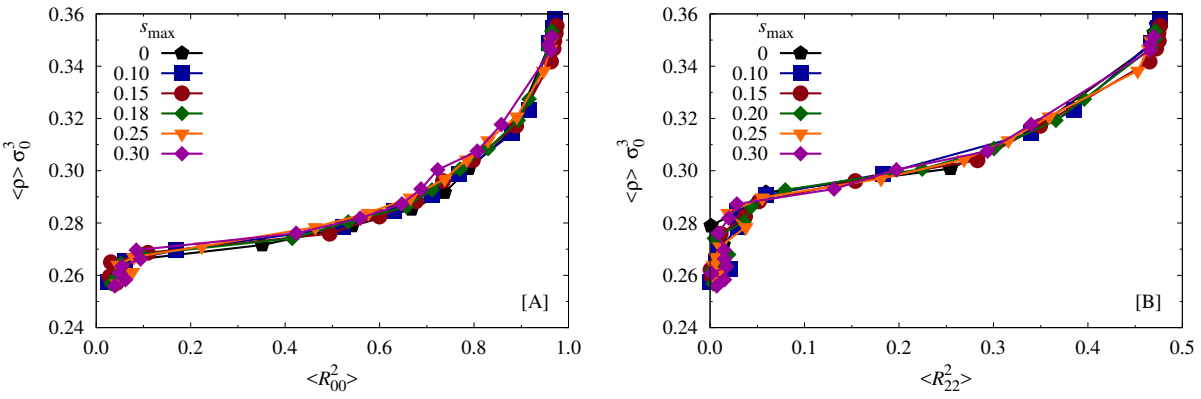


Figure S7: The average number density $\langle\rho\rangle$ plotted with respect to the $\langle R^2_{00}\rangle$ (plate A), and $\langle R^2_{22}\rangle$ (plate B) order parameters measured for the refernce ellipsoids with $s = 0.00$ in the five non–uniform mixtures. See caption of Figure S4 for further details.

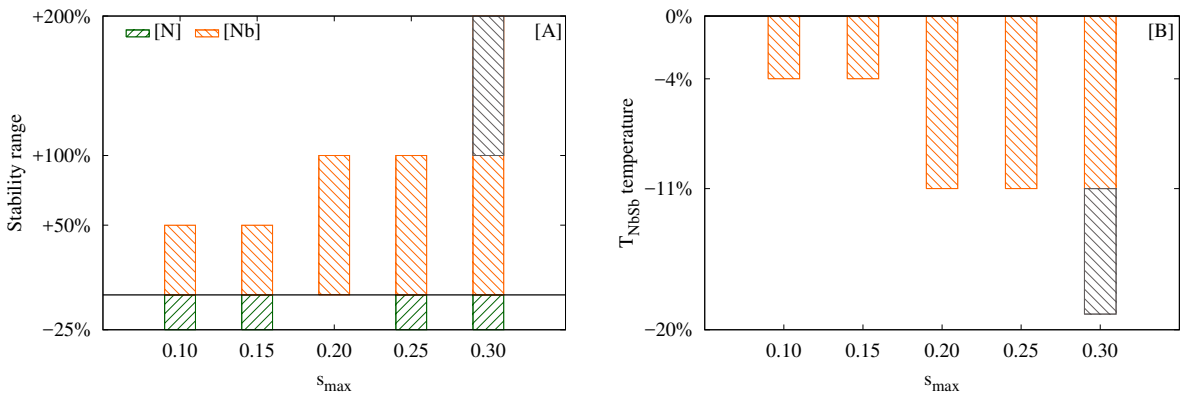


Figure S8: Pictorial representation of the changes in temperature stability ranges of the N and $N_b$ phases (plate A), and reduction of the $T^*_{NbSb}$ transition temperature (plate B) for the five non–uniform mixtures with respect to the reference system with $s_{max} = 0.00$.

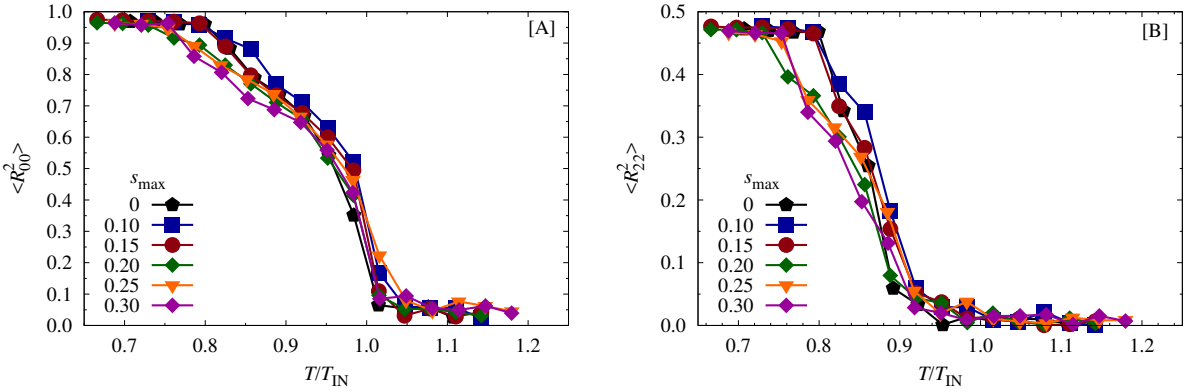


Figure S9: The average $\langle R^2_{00} \rangle$ (plate A), and $\langle R^2_{22} \rangle$ (plate B) order parameters for the reference ellipsoids with $s = 0.00$, at various reduced temperatures for the five non–uniform mixtures. See caption of Figure S4 for further details.

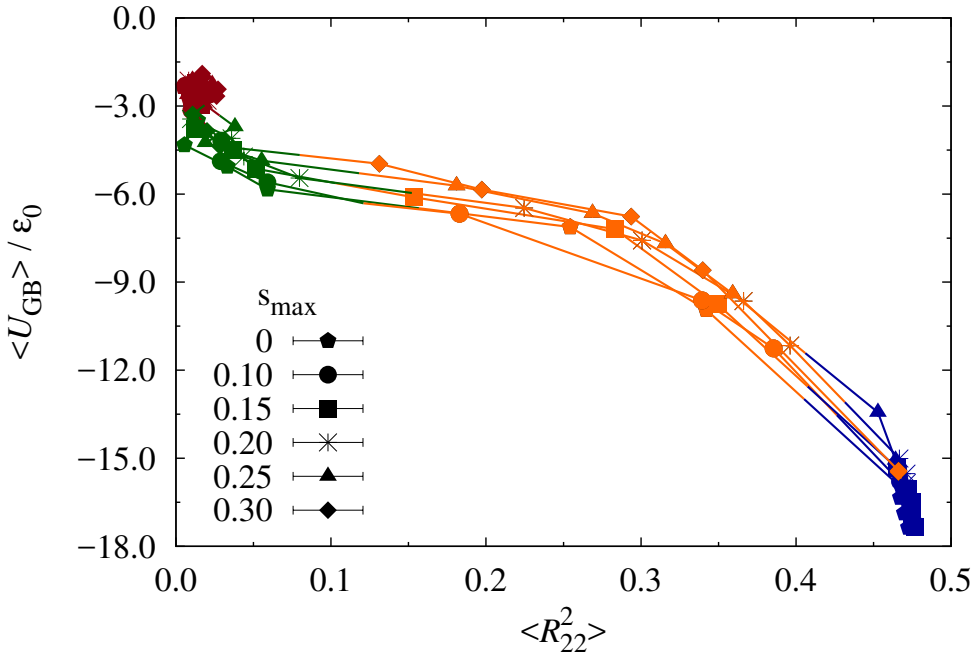


Figure S10: The average potential energy $\langle U_{\mathrm{GB}} \rangle$ plotted with respect to the $\langle R_{22}^2 \rangle$ order parameter measured for the refernce ellipsoids with $s = 0.00$ in the five non–uniform mixtures. See caption of Figure S4 for further details.